# Poly(ethylene glycol) cryogels as potential cell scaffolds: effect of polymerization conditions on cryogel microstructure and properties†

**Yongsung Hwang,[ab] Chao Zhang[b] and Shyni Varghese*[b]**

***Received 19th August 2009, Accepted 28th September 2009***
***First published as an Advance Article on the web 4th November 2009***
**DOI: 10.1039/b917142h**

We report the synthesis and characterization of interconnected macroporous network structures of poly(ethylene glycol) (PEG) using cryogelation techniques. Novel monolithic networks containing a gradient of pore size in a layered fashion were created from a single precursor by manipulating their polymerization kinetics. Maintaining conditions that promote the rate of gelation compared to that of the nucleation of ice crystals leads to formation of either conventional hydrogel-like network structures or continuous heterogeneous networks containing layers of hydrogel-like and cryogel-like microstructures. In contrast, conditions promoting a faster rate of the nucleation of ice crystals compared to rate of gelation result in cryogels with a nearly homogeneous interconnected macroporous network. The rates of polymerization and nucleation of ice crystals were altered using a number of different parameters such as concentration of initiator, freezing temperature, and degree of supercooling. Compared to conventional hydrogels, the cryogels exhibit higher stress and strain at break; their mechanical and equilibrium swelling properties show a strong correlation with the network microstructure. Cell viability studies suggest no detrimental effect of these scaffolds on cell attachment and their distribution. Furthermore, a time dependent increase in chondrocyte proliferation was observed in cryogels over a long period of culture.

## Introduction

Hydrogels are three-dimensional, insoluble, cross-linked networks of polymers that can imbibe large quantities of aqueous solutions. Hydrogels are excellent candidates for tissue engineering scaffolds because of their hydrophilic nature and mass transfer properties.[1,2] Factors affecting microstructure of the scaffolds such as pore size and interconnectivity of pores play an important role in determining cell proliferation, differentiation, and subsequent tissue formation. Macroporous hydrogels with interconnected pores not only provide sufficient surface area for cell attachment and proliferation but also allow enhanced mass transfer of oxygen, nutrients and waste removal.[3,4]

Various methods have been used in the past to produce macroporous hydrogels such as gas foaming,[4,5] fiber bonding,[6] micro-emulsion formation,[7] phase separation,[8] freeze-drying,[9] and porogen leaching.[10,11] More recently, cryogelation has been explored as a green process to synthesize three-dimensional (3D) hydrophilic structures with highly interconnected macroporous networks, termed cryogels. Cryogels are synthesized at subzero temperature where the reactants concentrated in the unfrozen/semi-frozen phase undergo polymerization to form a crosslinked network, while ice crystals start nucleating from the aqueous phase. These ice crystals function as porogens to produce interconnected macroporous network structures. The cryogels are characterized for their highly interconnected macroporous network structures with enhanced mechanical properties.[12,13]

Previously, there have been a few studies investigating the potential of cryogels as cell scaffolds. Kathuria *et al*. synthesized chitosan-gelatin cryogels and characterized their mechanical stability under various cyclic compressions. They also showed the cell viability and proliferation of fibroblasts within these cryogels.[14] Another study by Bolgen *et al*. reported the formation of 2-hydroxyethyl methacrylate (HEMA)-lactate-dextran cryogels, and their *in vitro* biocompatibility.[15] Beyond tissue engineering applications, cryogels have also been investigated in separation techniques.[16,17] Although these studies suggest the potential application of cryogels, a detailed characterization of cryogel structures has not been carried out as yet. One of the attractive features of cryogels is their network microstructure, and in this study we evaluate the parameters that affect the microstructure of cryogels using poly(ethylene glycol) (PEG) as a model system. The choice of PEG is based on its widespread use in tissue engineering and other biomedical applications. While PEG hydrogels have been extensively explored as cell scaffolds and delivery vehicles,[1,18–20] there have been no reports on formation and characterization of PEG cryogels.

Previous studies have demonstrated the effect of monomer concentration, degree of crosslinking, and solvent type on the pore structures of acrylamide cryogels.[21] Studies have also shown the effect of freezing temperature on the microstructure of cryogels.[22] In this study, we evaluate the role of polymerization rate on cryogel formation without altering the concentration of precursors/monomers or solvent. The cryogels were synthesized

[a]*Materials Science and Engineering Program, University of California at San Diego, 9500 Gilman Drive, La Jolla, CA92093-0418, USA*
[b]*Department of Bioengineering, University of California at San Diego, 9500 Gilman Drive, La Jolla, CA92093-0412, USA. E-mail: svarghese@ucsd.edu*

† Electronic supplementary information available: Thermograms, a photograph, SEM images and a stress–strain curve. See DOI: 10.1039/b917142h

using diacrylated PEG (PEGDA) as a precursor. The rate of polymerization/gelation was controlled by varying the concentration of TEMED (*N*,*N*,*N*′,*N*′-tetramethylethylenediamine), which functions as an accelerator in a redox initiator-mediated polymerization. We also investigated the effect of freezing temperature and degree of supercooling on cryogelation since these parameters have a significant effect on both the formation of ice crystals and the rate of gelation.

## Experimental

### Materials

Toluene and triethylamine were purchased from Fisher Scientific, and dichloromethane and diethyl ether were purchased from Sigma-Aldrich. Poly(ethylene glycol) (PEG) ($M_n$ 3400) and acryloyl chloride were purchased from Aldrich and they were used to synthesize poly(ethylene glycol) diacrylate (PEGDA) oligomer without any further purification. Ammonium persulfate (APS) and *N*,*N*,*N*′,*N*′-tetramethylethylenediamine (TEMED) were obtained from Sigma. For cell viability tests, a Live/Dead Viability/Cytotoxicity Kit (Molecular Probes, Cat#L-3224) was purchased from Molecular Probes.

### Synthesis of PEGDA oligomer

PEGDA oligomer was prepared according to the reported method.[23] Briefly, 18.0 g of PEG was dissolved in 300 mL of toluene in a 500 mL round bottomed flask in an oil bath heated at 125 °C. The solution was then refluxed for 4 h with vigorous stirring. Traces of water in the reaction mixture were removed by azeotropic distillation. Upon cooling the solution to room temperature, 3.262 g (32.2 mmol, 4.493 mL) of triethylamine was added to it with vigorous stirring. Then the flask was moved to an ice bath and stirred for 30 min. 2.918 g (32.2 mmol, 2.452 mL) of acryloyl chloride in 15 mL of anhydrous dichloromethane was then added to the reaction mixture dropwise over 30 min. After keeping the reaction mixture in the ice bath for another 30 min, the flask was heated at 45 °C overnight. The reaction mixture was then cooled to room temperature and the quaternary ammonium salt was removed from the reaction mixture by filtering through diatomaceous earth (2–3 cm) on a fritted glass funnel. The filtrate was condensed using a rotary evaporator and then precipitated in excess diethyl ether. The white precipitate was collected by filtration and vacuum dried at 40 °C for 24 h. The resultant PEGDA oligomer was purified by precipitation followed by column chromatography and dialysis prior to its usage.

### Synthesis of PEG cryogels

PEGDA oligomers were dissolved in phosphate buffered saline (PBS) to prepare a solution of 10% w/v. To this solution at 4 °C, the initiator–accelerator mixture {0.5% w/v of ammonium persulfate (APS) and either 0.05% or 0.1% w/v of *N*,*N*,*N*′,*N*′-tetramethylethylenediamine (TEMED)} was added, and the reaction mixture was polymerized at −14 °C or −20 °C for 20 h. Two cooling rates were used to evaluate the effect of degree of supercooling and onset of the nucleation of ice crystals on cryogel formation and microstructure.

### Characterization of PEG cryogels

**Scanning electron microscopy.** The microstructures of the PEG cryogels and hydrogels were examined using scanning electron microscopy (SEM, Philips XL30 ESEM). Briefly, the samples were dehydrated in 50%, 75% and 100% ethanol and dried using a critical point dryer (Tousimis AutoSamdri 815). After the samples were completely dried, they were gold-coated using a sputter coater (Emitech K575X Sputter Coater) for 30 s prior to SEM imaging.

**Swelling ratio measurement.** The swelling ratios of each sample were measured using a gravimetric method. After removing unreacted monomer by washing in excess water, cryogels were dried using a hot air sterilizer oven (Fisher Scientific 525D) at 60 °C, followed by a vacuum oven (Shel Lab 1410) until a constant dried weight was reached. Each sample was immersed in PBS at 37 °C for 48 h and their swollen weights were measured immediately after removal of excess water from the surface using a slightly wet tissue paper. The equilibrium swelling ratios of the samples were determined as a ratio of weights of equilibrium swollen gel to dried gel.[24]

**Mechanical testing.** Prior to compression testing, the cryogels were immersed in PBS for 24 h to reach equilibrium swelling. Compression tests were performed using an Instron 3342 Universal Testing System (Instron, Norwood, MA, USA) equipped with a Model 2519-104 force transducer. Samples were compressed with two parallel plates at the maximum loading of 250 N with a compression rate of 1 mm $min^{-1}$. The compressive modulus was calculated from the linear region of the stress–strain curve (0–10% strain). All measurements were carried out in quadruplicate for each set of parameters.

### Cryogels as cell scaffolds

The potential application of PEG cryogels as cell scaffolds has been evaluated using bovine chondrocytes (bCCs) and human mesenchymal stem cells (hMSCs). Prior to seeding cells, cryogels were sterilized with 70% ethanol and were washed with fresh PBS. The rinsed cryogels were coated with collagen type I solution (50 μg $mL^{-1}$, BD Bioscience, Cat# 354231) to improve cell adhesion prior to cell seeding. The cells were seeded onto the cryogels at a seeding density of $1 \times 10^6$ cells/cryogel. The cell-loaded cryogels having dimensions of 10 mm diameter and 5 mm height were incubated in a growth medium (Dulbecco's Modified Eagle Medium (DMEM) containing 10% fetal bovine serum (FBS)).

### Cell viability test

A Live/Dead assay was performed to evaluate the cell viability after 36 h of cell seeding.[25] Briefly, cell-laden cryogels were cut into thin slices and incubated with the Live/Dead assay dye solution (Molecular Probes, Cat# L-3224), which contained 0.5 μL of Calcein-AM and 2 μL of ethidium homodimer-1 in 1 mL of DMEM. After 30 min of incubation, the slices were rinsed with PBS and images were obtained using a fluorescence microscope.

### Statistical analysis

All data are presented as mean ± standard deviation (SD). Single factor analysis of variance (ANOVA) was performed to determine statistical significance ($p < 0.05$).

## Results and discussion

### Influence of polymerization conditions on cryogel structures

PEG cryogels were synthesized by radical polymerization of PEGDA having a molecular weight ($M_n$) of 3400 using redox initiators APS/TEMED. In this study, we have used two different concentrations of TEMED, 0.05% and 0.1% w/v, to vary the rate of polymerization. Previous studies have demonstrated that a high concentration of redox initiators in the reaction mixture enhances their rate of polymerization.[22,26] In addition to TEMED concentration, we have also varied temperatures of cryogelation (−14 °C and −20 °C), and degree of supercooling. We have chosen to vary the freezing temperature and degree of supercooling as they play a critical role in determining the network structure of cryogels due to their influence on both formation of the polymer network and ice crystals.[21]

First the effect of TEMED mediated polymerization rate on formation of cryogels and their network structure was studied by varying the concentration of TEMED in the reaction mixture. Varying the rate of polymerization resulted in PEG cryogels with different microstructures. The PEGDA reaction mixture containing 0.1% w/v TEMED upon thawing after 20 h at −20 °C formed a crosslinked network. The physical appearance of these networks along with their swelling/deswelling behavior suggests that they exhibit a heterogeneous microstructure. Our first observation was that only the top regions of these cryogels exhibited rapid absorption and release of water molecules, while maintaining a different swelling behavior for the bottom region. Additionally, at equilibrium swollen state these cryogels showed a heterogeneous shape—an expanded top region with a higher diameter compared to the bottom region (Fig. 1a). The heterogeneous structure of these cryogels synthesized at −20 °C became more apparent in their dried state (Fig. 1b). These observations clearly suggest a heterogeneous network structure in which the top layer has a highly interconnected macroporous structure (cryogel-like structure) while the bottom layer has a closed network structure with small pores (hydrogel-like structure). Hereafter we refer to these heterogeneous cryogels as $I_{0.1}T_{-20}C_S$, where $I_{0.1}$ represents the amount of TEMED, $T_{-20}$ represents the freezing temperature and $C_S$ represents the slow cooling rate. The nomenclature used for various cryogels discussed in this study is tabulated in Table 1. The layered heterogeneous network

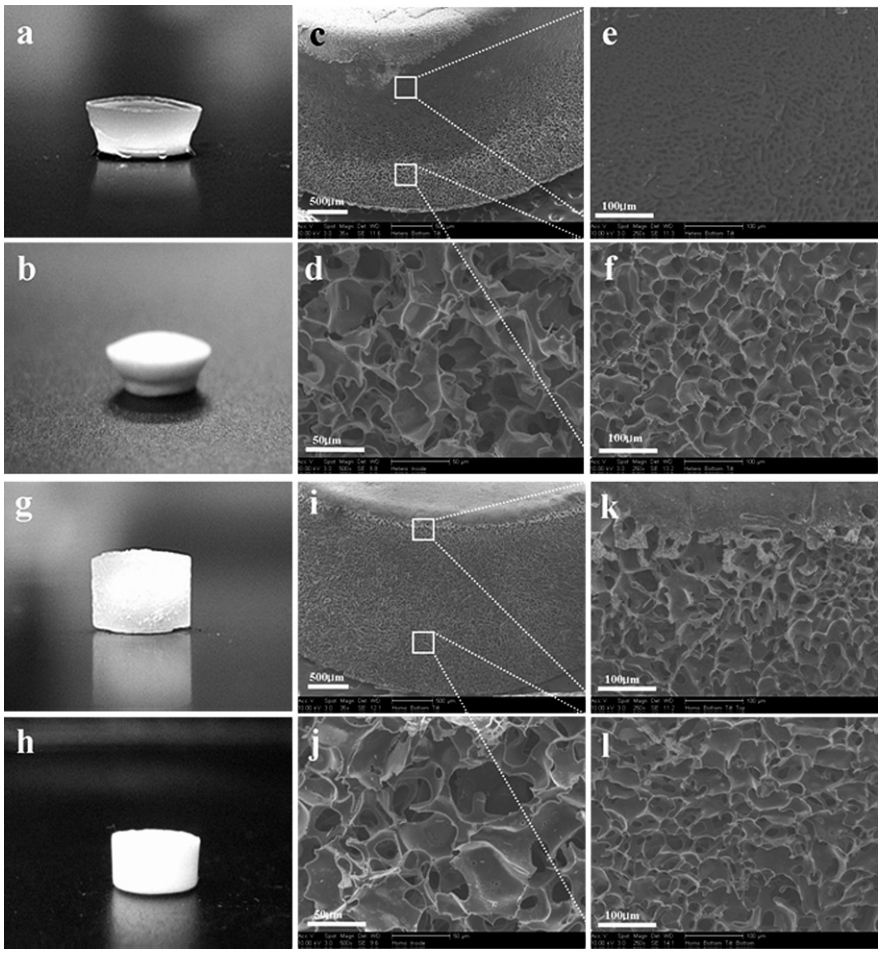


**Fig. 1** Photographs (a, b, g, h) and SEM images (c–f, i–l) of heterogeneous cryogel ($I_{0.1}T_{-20}C_S$) (a–f) and homogeneous cryogel ($I_{0.05}T_{-20}C_S$) (g–l): (a, g) equilibrium swollen cryogels; (b, h) dried cryogels; (c, i), (e, f, k, l) side view of cryogels; and (d, j) internal fracture surface of cryogels.

**Table 1** Compositions and nomenclature of the cryogels

| Sample code | Amount (w/v) of TEMED | *Temp.*/°C of polymerization | Rate of cooling |
|---|---|---|---|
| $I_{0.1}T_{-14}C_F$ | 0.1% | −14 | Fast |
| $I_{0.1}T_{-20}C_F$ | 0.1% | −20 | Fast |
| $I_{0.1}T_{-20}C_S$ | 0.1% | −20 | Slow |
| $I_{0.05}T_{-14}C_F$ | 0.05% | −14 | Fast |
| $I_{0.05}T_{-20}C_F$ | 0.05% | −20 | Fast |
| $I_{0.05}T_{-20}C_S$ | 0.05% | −20 | Slow |
| Conventional hydrogels | 0.05% | 20 | N/A |

structure of $I_{0.1}T_{-20}C_S$ was further confirmed by scanning electron microscopy (SEM) analysis (Fig. 1c–f). Fig. 1c and 1e–f show the side view of the $I_{0.1}T_{-20}C_S$ cryogel containing both cryogel-like and hydrogel-like structures within the same network, while Fig. 1d shows their internal network structure.

In contrast, PEGDA reaction mixtures containing low amounts of TEMED concentration (0.05% w/v) resulted in a homogeneous network structure as indicated by their physical appearance and swelling behavior (Fig. 1g, h). These cryogels (referred to as $I_{0.05}T_{-20}C_S$) showed homogeneous swelling in PBS solution unlike their heterogeneous counterparts, $I_{0.1}T_{-20}C_S$. SEM analysis of these cryogels showed highly interconnected macroporous structures with pore sizes ranging 30–100 μm throughout the network (Fig. 1i). These pore sizes are slightly higher than those observed in $I_{0.1}T_{-20}C_S$ cryogels which have pore sizes in the range of 30–70 μm in the cryogel layer. Fig. 1i–l show the internal network structures and the side view of $I_{0.05}T_{-20}C_S$. As seen from Fig. 1c, i, a thin layer of hydrogel of the order of 5–10 μm at the bottom of the cryogel adjacent to the plastic mold was always observed irrespective of the experimental conditions. The corresponding thermogram for the cryogelation at −20 °C is shown in the ESI, Fig. S1a,† which shows that the cryogelation of $I_{0.05}T_{-20}C_S$ involved a degree of supercooling of 10.9 °C with an onset of nucleation of ice after 12 min of incubation.

The formation of a heterogeneous network at high TEMED concentration could be explained based on a competition between the rate of nucleation of ice crystals and the rate of gelation. The process of cryogelation involves polymerization/gelation of the reaction mixture (unfrozen liquid phase containing high concentration of reactants) and the nucleation of ice crystals; the microstructures of cryogels are strongly dependent upon the kinetics of these two processes.[14,21] In the case of heterogeneous cryogels, the presence of hydrogel-like structure is a result of the gelation process proceeding at a faster rate than the nucleation of ice crystals.

The tight network formed due to faster gelation prevents distribution of the ice crystals formed, which act as porogens to produce macroporous and interconnected pore structures throughout the gel network. As a result, the few ice crystals formed float on the top due to their lower density compared to the liquid phase, thus yielding a layered network structure comprising of a cryogel-like structure on the top and a hydrogel-like structure at the bottom.

Since the degree of supercooling and onset of nucleation of ice crystals have critical roles in determining the microstructure of cryogels, we evaluated the effect of these parameters on the microstructure of cryogels synthesized at −20 °C. As seen from the ESI, Fig. S1b,† we have used a faster cooling rate compared to the one described above for creating $I_{0.1}T_{-20}C_S$ and $I_{0.05}T_{-20}C_S$. The thermogram exhibits a degree of supercooling of 16.3 °C and the nucleation of ice initiates at around 1.5 min after their incubation (Fig. S1b†). Irrespective of the faster cooling, the precursors containing higher amounts of TEMED again resulted in a heterogeneous cryogel exhibiting a layer of cryogel-like structure at the top and another layer of hydrogel-like structure at the bottom similar to $I_{0.1}T_{-20}C_S$ (ESI, Fig. S2†). We refer to these cryogels as $I_{0.1}T_{-20}C_F$, where $C_F$ indicates a faster cooling rate. A close observation of the resulting cryogels indicates that the hydrogel layer of $I_{0.1}T_{-20}C_F$ is thinner as compared to $I_{0.1}T_{-20}C_S$. SEM analysis of the $I_{0.1}T_{-20}C_F$ cryogel also shows a different internal structure where the cryogel-like structure exhibits a much smaller pore size (20–40 μm) as compared to $I_{0.1}T_{-20}C_S$. A similar trend was observed in the case of cryogels synthesized using low TEMED concentration, where the internal structure of these homogeneous cryogels, $I_{0.05}T_{-20}C_F$, showed a more interconnected network structure with a pore size of 20–50 μm (ESI, Fig. S3–S4†). The smaller pore size could be attributed to the higher degree of supercooling, which results in ice crystals with smaller sizes.

Having established the effect of the rate of gelation and degree of supercooling on cryogelation and their microstructure, we then evaluated the effect of freezing temperature on cryogel formation using two temperatures: −14 °C and −20 °C. The reaction mixtures containing 0.1% w/v TEMED failed to form a cryogel at −14 °C, unlike −20 °C, but instead formed a conventional hydrogel-like structure (Fig. 2a). However, reaction mixtures containing low TEMED concentrations (0.05% w/v) resulted in cryogels with homogeneous network structures at −14 °C as shown in Fig. 2b. Fig. 2e, f show the side view of this homogeneous cryogel, $I_{0.05}T_{-14}C_F$. The pore sizes were observed to be in the range of 30–100 μm and were bigger than those of $I_{0.05}T_{-20}C_F$, but they were very similar to those of $I_{0.05}T_{-20}C_S$ (Fig. 2c). The similar pore size observed between $I_{0.05}T_{-14}C_F$ and $I_{0.05}T_{-20}C_S$ could be attributed to their similar degree of supercooling (12 °C) and the corresponding thermogram for $I_{0.05}T_{-14}C_F$ is shown in the ESI, Fig. S1c.† One of the significant differences between the cryogels formed at −14 °C and −20 °C ($I_{0.05}T_{-14}C_F$ and $I_{0.05}T_{-20}C_F$) is that the former appeared to have somewhat closed or disconnected structures while the latter showed continuous interconnected microstructures (Fig. 2d and ESI, Fig. S4a†).

### Swelling properties of cryogels

The synthesis of macroporous network structures has been adopted previously to improve the swelling–deswelling kinetics of various hydrogels.[27,28] As seen from Fig. 3, the homogeneous cryogels, $I_{0.05}T_{-20}C_S$ and $I_{0.05}T_{-14}C_F$, undergo faster swelling kinetics than conventional hydrogels which show a gradual swelling over the time. These homogeneous cryogels ($I_{0.05}T_{-20}C_S$ and $I_{0.05}T_{-14}C_F$), irrespective of their differences in cryogelation procedure, had similar equilibrium swelling and exhibited similar swelling kinetics (Table 2 and Fig. 3). The cryogels reached equilibrium swelling within 1–2 min. In contrast, corresponding

 

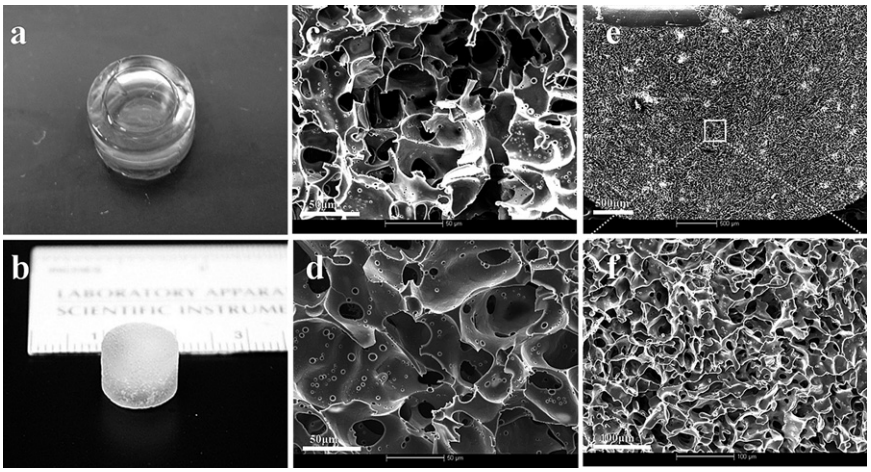


**Fig. 2** Photographs (a, b) and SEM images (c–f) of hydrogels and homogeneous cryogels: (a) equilibrium swollen network, synthesized at −14 °C using 0.1% w/v TEMED, exhibiting a hydrogel like appearance; (b) equilibrium swollen homogeneous cryogel ($I_{0.05}T_{-14}C_F$), synthesized at −14 °C using 0.05% w/v TEMED; (c) internal fracture surface of $I_{0.05}T_{-14}C_F$ exhibiting interconnected pores; and (d) internal fracture surface of $I_{0.05}T_{-14}C_F$ showing a closed pore structure; (e, f) side view of $I_{0.05}T_{-14}C_F$.

conventional hydrogels synthesized at room temperature took almost 12 h to reach the equilibrium swelling and showed much smaller equilibrium swelling ratios than homogeneous cryogels (Table 2). The equilibrium swelling ratios of heterogeneous cryogels, $I_{0.1}T_{-20}C_S$, were found to be higher than conventional hydrogels but lower than homogeneous cryogels ($I_{0.05}T_{-20}C_S$ and $I_{0.05}T_{-14}C_F$). Further probing of the swelling kinetics of heterogeneous cryogels, $I_{0.1}T_{-20}C_S$, showed that they exhibit a two step swelling. Upon immersion of dried $I_{0.1}T_{-20}C_S$ in PBS solution, the cryogel-like top region was found to undergo rapid swelling, while the hydrogel-like bottom region underwent slow swelling. To further clarify this, we dissected the two layers of these heterogeneous cryogels and evaluated their swelling independently. Indeed the cryogel-like top structure showed a rapid swelling, characteristic of a macroporous cryogel structure, while the bottom layer having a hydrogel-like structure showed slower swelling similar to the conventional hydrogels. Therefore, the observed swelling behavior of heterogeneous cryogels is a combination of swelling behaviors from cryogel-like and hydrogel-like structures.

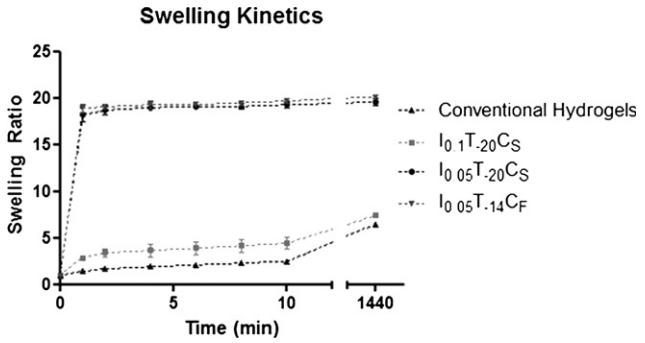


**Fig. 3** Swelling kinetics of conventional hydrogels, and the heterogeneous ($I_{0.1}T_{-20}C_S$) and homogeneous cryogels ($I_{0.05}T_{-20}C_S$ and $I_{0.05}T_{-14}C_F$). (From $t = 1$ min to $t = 1440$ min, * $p < 0.05$ for all cryogels compared to conventional hydrogels; ** $p < 0.05$ for comparison between $I_{0.05}T_{-20}C_S$ and $I_{0.1}T_{-20}C_S$ for whole period of time).

## Mechanical properties of cryogels

We then evaluated the effect of network microstructure on mechanical properties. Compared to conventional hydrogels, heterogeneous and homogeneous cryogels exhibited lower compressive moduli (Table 2). Among the homogeneous cryogels, $I_{0.05}T_{-14}C_F$ had a higher compressive modulus than that of $I_{0.05}T_{-20}C_S$. The compressive moduli of these cryogels were very close to those of heterogeneous cryogels, $I_{0.1}T_{-20}C_S$. Conventional hydrogels showed 53.74% of deformation and 0.14 MPa of maximum stress, thereby exhibiting brittle mechanical properties. In contrast, heterogeneous and homogeneous cryogels showed larger deformations and fracture stress (Table 2). The $I_{0.05}T_{-14}C_F$ cryogels exhibited a deformation of 85.86% and a fracture stress of 1.30 MPa, whereas deformation and fracture stress of $I_{0.05}T_{-20}C_S$ cryogels were measured to be 91.70% and

**Table 2** Mechanical properties of conventional hydrogels, heterogeneous ($I_{0.1}T_{-20}C_S$) and homogeneous cryogels ($I_{0.05}T_{-20}C_S$ and $I_{0.05}T_{-14}C_F$)

| Entry | Toughness/kJ $m^{-3}$ | Stress at break/MPa | Strain at break (%) | Compressive modulus/kPa | Equilibrium swelling ratio |
|---|---|---|---|---|---|
| Conventional hydrogel | 21.93 ± 5.50 | 0.14 ± 0.04 | 53.74 ± 4.02 | 57.04 ± 3.48 | 6.49 ± 0.17 |
| $I_{0.1}T_{-20}C_S$ | 38.95 ± 12.33[b,c] | 0.39 ± 0.14[b,c] | 72.94 ± 9.24[a,c] | 24.17 ± 3.16[a,d] | 7.43 ± 0.26[a,c] |
| $I_{0.05}T_{-20}C_S$ | 71.33 ± 9.12[a,c] | 1.62 ± 0.16[a,c] | 91.70 ± 0.64[a,c] | 18.60 ± 1.13[a,d] | 19.60 ± 0.42[a,c] |
| $I_{0.05}T_{-14}C_F$ | 61.64 ± 7.34[a] | 1.30 ± 0.19[a] | 85.86 ± 1.17[a] | 25.60 ± 1.33[a] | 20.14 ± 0.07[a] |

[a] $p < 0.05$ for $I_{0.05}T_{-20}C_S$ and $I_{0.05}T_{-14}C_F$ compared to conventional hydrogels. [b] $p > 0.05$ for comparison between $I_{0.1}T_{-20}C_S$ and conventional hydrogels. [c] $p < 0.05$ for comparison between $I_{0.05}T_{-20}C_S$ and $I_{0.1}T_{-20}C_S$. [d] $p > 0.05$ for comparison between $I_{0.05}T_{-20}C_S$ and $I_{0.1}T_{-20}C_S$.

1.62 MPa, respectively. The $I_{0.1}T_{-20}C_S$ cryogels exhibited a large deformation of up to 72.94% with a fracture stress of 0.39 MPa. The higher compressive modulus of $I_{0.05}T_{-14}C_F$ cryogels over $I_{0.05}T_{-20}C_S$ could be attributed to their closed macroporous network structure. The higher compressive modulus of $I_{0.1}T_{-20}C_S$ could be attributed to the hydrogel like structure of the bottom region of these cryogels. During the mechanical measurements, we consistently observed that the cracks were initiated at the hydrogel-like layer and not at the cryogel-like layer. While the hydrogel-like structure contributes to the higher compressive modulus of heterogeneous cryogels, the cryogel-like structure contributes to their larger deformations, which were lower than those of homogeneous cryogels ($I_{0.05}T_{-20}C_S$ and $I_{0.05}T_{-14}C_F$) but significantly higher than that of conventional hydrogels.

The equilibrium swollen cryogels were easily compressed, during which the cryogels expelled the imbibed PBS. The rapid deswelling of these networks under stress is attributed to their highly interconnected macroporous structure. In the case of heterogeneous cryogels, rapid deswelling was observed only in the top region while the bottom region retained the imbibed water (data not shown).

### Cytocompatibility of cryogels

In order to investigate the potential of the PEG cryogels as cell scaffolds for tissue engineering, we evaluated the response of cells to the scaffold using both bovine chondrocytes (bCCs) and human mesenchymal stem cells (hMSCs). As seen in Fig. 4a, the PEG cryogels coated with collagen type I provided structural support for the attachment of chondrocytes and most of the chondrocytes were viable after 36 h of culture. The seeded cells migrated and homogeneously distributed within the homogeneous cryogels like $I_{0.05}T_{-20}C_S$. A similar behavior was observed in the case of hMSCs (data not shown). In the case of heterogeneous cryogels ($I_{0.1}T_{-20}C_S$), the cells were found to be confined within the cryogel layer, unlike homogenous cryogels where the cells were distributed within the entire network. The distribution of seeded cells within the cryogels was observed even in the absence of collagen type 1 coating. However, the number of cells distributed after 36 h of cell seeding was found to be lower than that of the corresponding collagen type 1 coated cryogels. As seen from Fig. 4b, a time dependent increase in chondrocyte proliferation was observed in cryogels, and it could be due to the high surface area and available pore size.

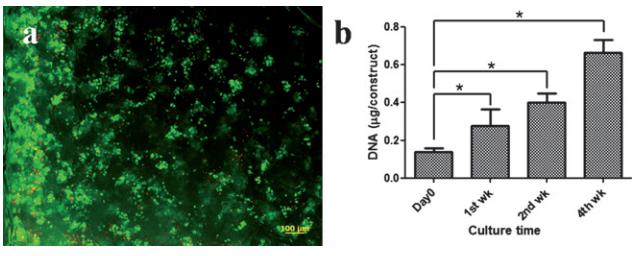


**Fig. 4** (a) Live/Dead assay of chondrocyte-loaded cryogel ($I_{0.05}T_{-20}C_S$) after 36 h of cell seeding. (b) Results of DNA assay showing the amount of DNA with culture time using $I_{0.1}T_{-20}C_S$ cryogels as cell scaffolds. (* $p < 0.05$ for 1st, 2nd and 4th week of DNA amount compared to Day 0).

## Conclusion

PEG cryogels with similar chemical composition but distinctly different microstructures were synthesized by manipulating the kinetics of polymerization. The effect of freezing temperature and degree of supercooling on cryogel formation and microstructure was also evaluated. We showed for the first time that monolithic heterogeneous networks containing both cryogel-like and hydrogel-like structures can be synthesized using cryogelation techniques by manipulating the polymerization kinetics. The ability to control the microstructure of cryogels *via* concentration of the initiator (accelerator) introduces a new handle to manipulate the structural properties of such materials. We also found that the mechanical and swelling properties of the cryogels were strongly dependent upon their network microstructure. These highly elastic interconnected macroporous structures could undergo large deformation without altering their structural properties. The tunable structural and mechanical properties, high elasticity, and swelling behavior favoring enhanced mass transport of PEG cryogels, along with their ability to support cell growth make them excellent scaffolds for cell and tissue engineering.

## Acknowledgements

The authors thank Professor Marc Meyers in the Department of Mechanical and Aerospace Engineering, University of California, San Diego for his assistance with mechanical testing and Dr Sangaj for helpful discussion. The authors also acknowledge Ryan Anderson for his assistance with the use of the SEM facility of Calit2 at the University of California, San Diego.

## References

1 S. Varghese and J. H. Elisseeff, *Adv. Polym. Sci.*, 2006, **203**, 95–144.
2 A. S. Hoffman, *Adv. Drug Delivery Rev.*, 2002, **43**(1), 3–12.
3 M. C. Peters and D. J. Mooney, *Porous Materials for Tissue Engineering*, 1997, **250**, 43–52.
4 B. S. Kim and D. J. Mooney, *Trends Biotechnol.*, 1998, **16**(5), 224–230.
5 D. J. Mooney, D. F. Baldwin, N. P. Suh, J. P. Vacanti and R. Langer, *Biomaterials*, 1996, **17**(14), 1417–1422.
6 A. G. Mikos, Y. Bao, L. G. Cima, D. E. Ingber, J. P. Vacanti and R. Langer, *J. Biomed. Mater. Res.*, 1993, **27**(2), 183–189.
7 D. J. Bennett, R. P. Burford, T. P. Davis and H. J. Tilley, *Polym. Int.*, 1995, **36**(3), 219–226.
8 Y. S. Nam and T. G. Park, *Biomaterials*, 1999, **20**(19), 1783–1790.
9 F. J. O'Brien, B. A. Harley, I. V. Yannas and L. J. Gibson, *Biomaterials*, 2005, **26**(4), 433–441.
10 A. G. Mikos, A. J. Thorsen, L. A. Czerwonka, Y. Bao, R. Langer, D. N. Winslow and J. P. Vacanti, *Polymer*, 1994, **35**(5), 1068–1077.
11 A. G. Mikos, G. Sarakinos, S. M. Leite, J. P. Vacanti and R. Langer, *Biomaterials*, 1993, **14**(5), 323–330.
12 F. M. Plieva, I. Y. Galaev, W. Noppe and B. Mattiasson, *Trends Microbiol.*, 2008, **16**(11), 543–551.
13 V. I. Lozinsky, I. Y. Galaev, F. M. Plieva, I. N. Savina, H. Jungvid and B. Mattiasson, *Trends Biotechnol.*, 2003, **21**(10), 445–451.
14 N. Kathuria, A. Tripathi, K. K. Kar and A. Kumar, *Acta Biomater.*, 2009, **5**(1), 406–418.
15 N. Bolgen, Y. Yang, P. Korkusuz, E. Guzel, A. J. El Haj and E. Piskin, *Tissue Eng., Part A*, 2008, **14**, 1743–1750.
16 P. Arvidsson, F. M. Plieva, V. I. Lozinsky, I. Y. Galaev and B. Mattiasson, *J. Chromatogr., A*, 2003, **986**(2), 275–290.
17 F. M. Plieva, J. Andersson, I. Y. Galaev and B. Mattiasson, *J. Sep. Sci.*, 2004, **27**(10–11), 828–836.
18 S. J. Bryant and K. S. Anseth, *J. Biomed. Mater. Res.*, 2002, **59**(1), 63–72.

 

19 S. J. Bryant, T. T. Chowdhury, D. A. Lee, D. L. Bader and K. S. Anseth, *Ann. Biomed. Eng.*, 2004, **32**(3), 407–417.
20 S. J. Bryant, C. R. Nuttelman and K. S. Anseth, *Biomed. Sci. Instrum.*, 1999, **35**, 309–314.
21 F. Plieva, X. Huiting, I. Y. Galaev, B. Bergenstahl and B. Mattiasson, *J. Mater. Chem.*, 2006, **16**(41), 4065–4073.
22 K. Yao, S. Shen, J. Yun, L. Wang, X. He and X. Yu, *Chem. Eng. Sci.*, 2006, **61**(20), 6701–6708.
23 D. L. Hern and J. A. Hubbell, *J. Biomed. Mater. Res.*, 1998, **39**(2), 266–276.
24 V. S. Bhalerao, S. Varghese, A. K. Lele and M. V. Badiger, *Polymer*, 1998, **39**(11), 2255–2260.
25 N. S. Hwang, S. Varghese and J. Elisseeff, *Methods Mol. Biol.*, 2007, **407**, 351–373.
26 S. Duan, W. Zhu, L. Yu and J. Ding, *Chin. Sci. Bull.*, 2005, **50**(11), 1093–1096.
27 J. Chen and K. Park, *J. Macromol. Sci., Part A: Pure Appl. Chem.*, 1999, **36**(7), 917–930.
28 N. Bolgen, F. Plieva, I. Y. Galaev, B. Mattiasson and E. Piskin, *J. Biomater. Sci., Polym. Ed.*, 2007, **18**(9), 1165–1179.

# Electronic Supplementary Information

## Poly(ethylene glycol) cryogels as potential cell scaffolds: Effect of polymerization conditions on cryogel microstructure and properties

Yongsung Hwang[a, b], Chao Zhang[b], and Shyni Varghese[b, *]

[a]Materials Science and Engineering Program, University of California at San Diego, 9500 Gilman Drive, La Jolla, CA92093-0418 (USA),

[b]Department of Bioengineering, University of California at San Diego, 9500 Gilman Drive, La Jolla, CA92093-0412 (USA)

[*]To whom correspondence should be addressed. E-mail: svarghese@ucsd.edu.

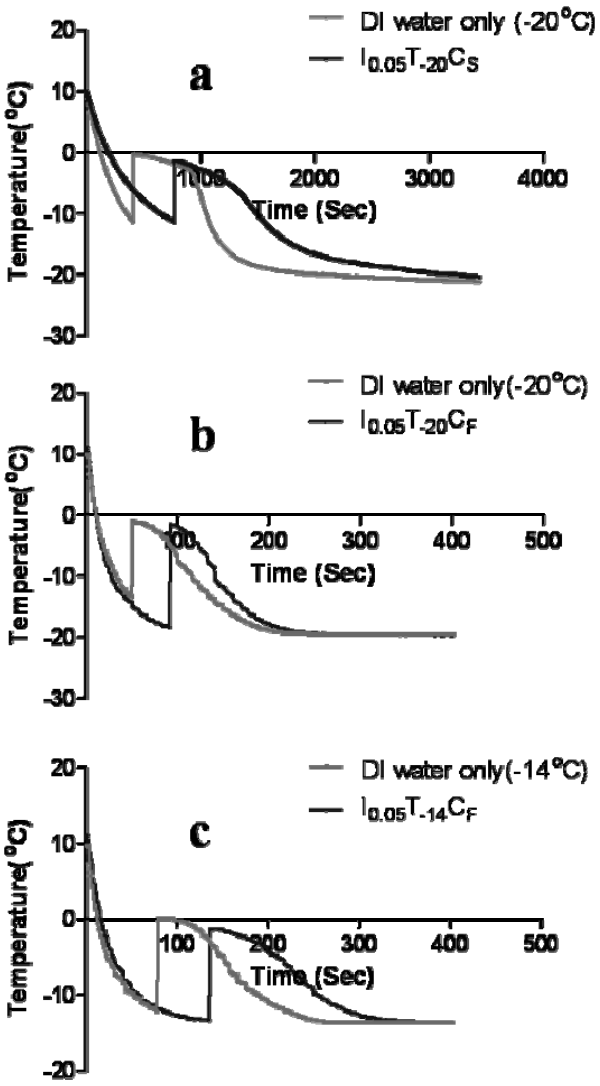


**Fig. S1** Thermograms of cryogelation at different temperatures with reference to DI water. (a) $I_{0.05}T_{-20}C_S$ (b) $I_{0.05}T_{-20}C_F$ (c) $I_{0.05}T_{-14}C_F$.

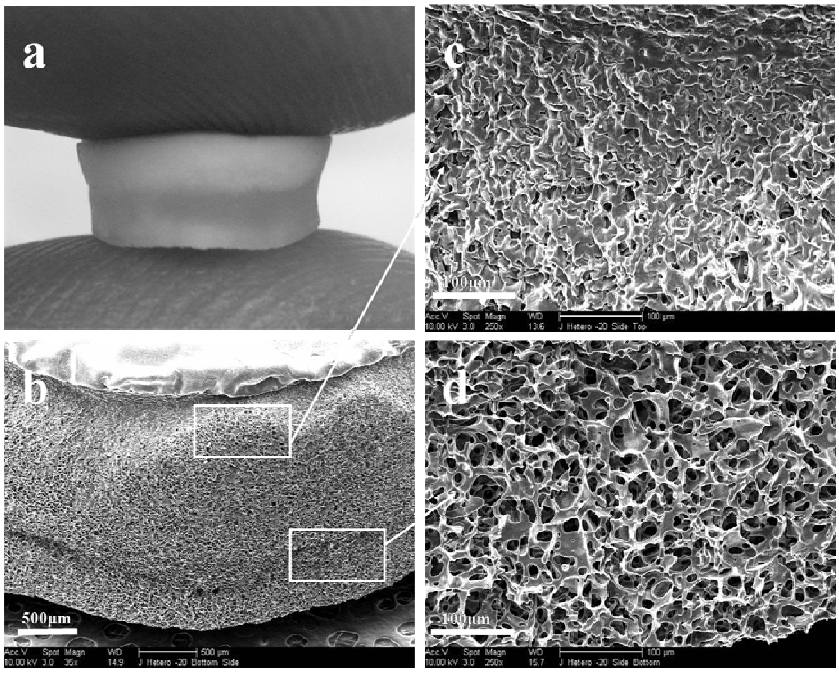


**Fig. S2** Photograph (a) and SEM images (b-d) of $I_{0.1}T_{-20}C_F$

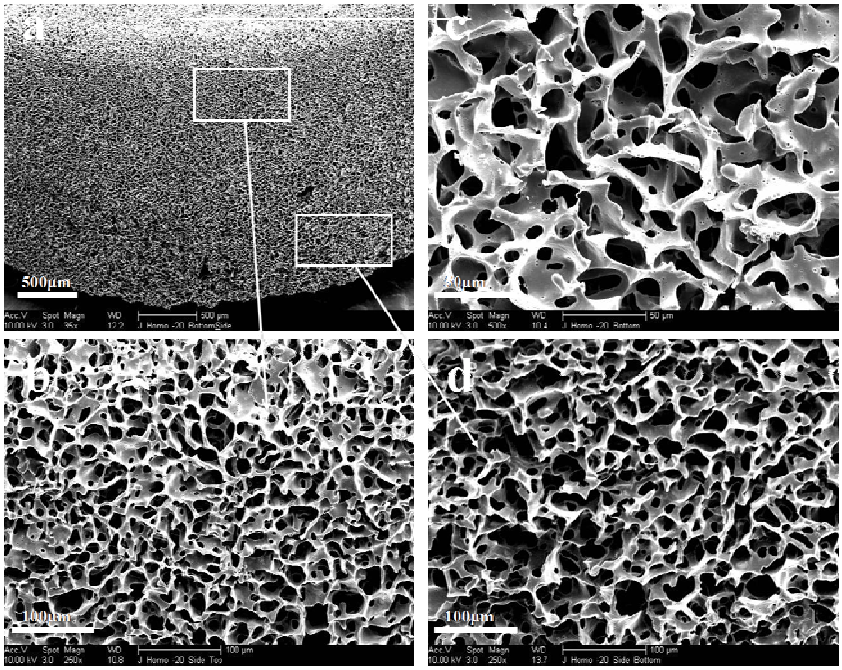


**Fig. S3** SEM images of bottom and side view of $I_{0.05}T_{-20}C_F$

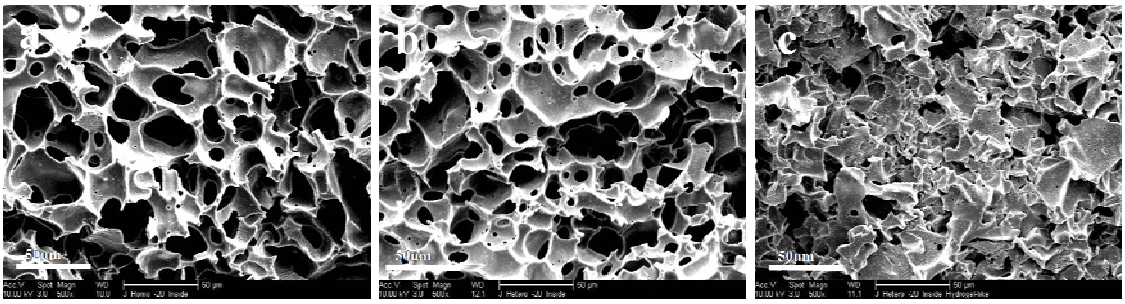


**Fig. S4** SEM images of $I_{0.05}T_{-20}C_F$ and $I_{0.1}T_{-20}C_F$; (a) internal fracture surface of $I_{0.05}T_{-20}C_F$, (b) internal fracture surface of cryogel-like structure of $I_{0.1}T_{-20}C_F$, and (c) internal fracture surface of hydrogel-like structure of $I_{0.1}T_{-20}C_F$.

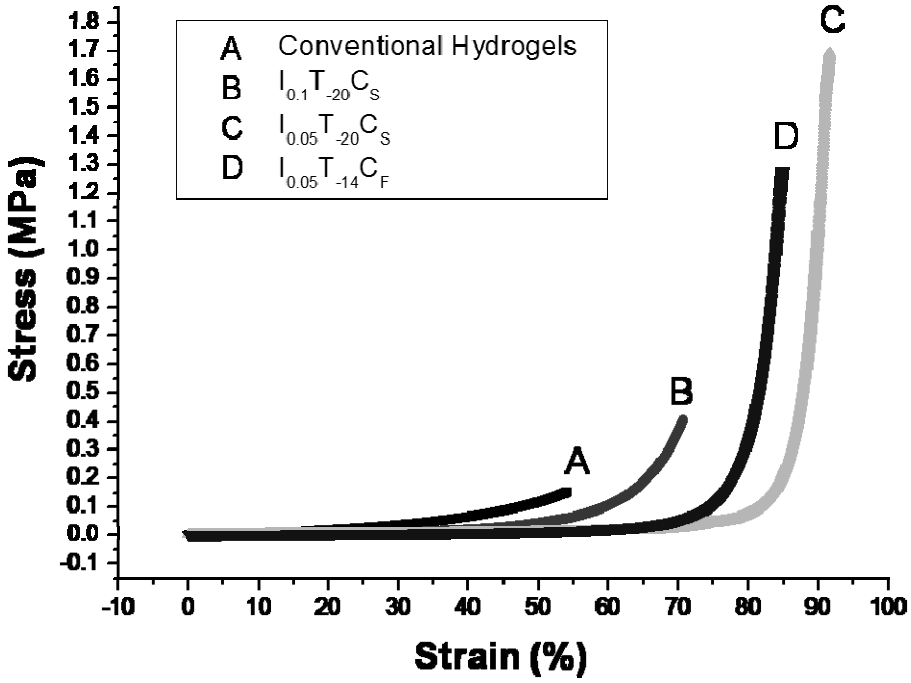


**Fig. S5** Stress-strain curves of conventional hydrogels, heterogeneous ($I_{0.1}T_{-20}C_S$) and homogeneous cryogels ($I_{0.05}T_{-20}C_S$ and $I_{0.05}T_{-14}C_F$).